

# DUAL ABRIKOSOV VORTICES IN CONFINING THEORIES

Richard W. Haymaker

*Department of Physics and Astronomy, Louisiana State University  
Baton Rouge, Louisiana, 70803, USA  
E-mail: haymaker@rouge.phys.lsu.edu*

## ABSTRACT

The spacial distribution of fields and currents in confining theories can give direct evidence of dual superconductivity. We would like to discuss the techniques for finding these properties and calculating the superconductivity parameters in lattice simulations. We have seen dual Abrikosov vortices directly in pure U(1) and SU(2) and others have also seen them in SU(3). In the non-Abelian cases the system appears to be near the borderline between type I and II. We also discuss the response of the supercurrents to external fields.

## 1. Introduction

Lattice gauge theory offers the prospect of exploring dual superconductivity<sup>1</sup> in depth as a confining mechanism. The existence of a dual Abrikosov vortex between a static quark-antiquark pair leads to a linearly rising potential energy between them and hence confinement. These have been seen in U(1), SU(2) and SU(3) lattice gauge simulations thereby supporting this picture of confinement.

In ordinary superconductivity, the primary issue is the spontaneous breaking of the electromagnetic U(1) gauge symmetry (SSB) signaled by the non-vanishing of the vacuum expectation value of a charged field. An immediate consequence is that the curl of the vector potential is proportional to the curl of the electric current known as the London relation. The London relation is violated only near the boundaries of superconducting material within a distance of the order of the coherence length. Combining the London relation with Maxwell's equations gives mass to the electromagnetic field. The Meissner effect and infinite conductivity follow.

The theory of superconductivity entails (i) the identification of what symmetry is broken and what are the relevant coordinates, (ii) the mechanism that leads to the instability and hence SSB, e.g. BCS theory, and then (iii) an effective theory of the currents and fields in the broken phase, e.g. Ginzburg-Landau [GL] theory, which predicts the spatial consequences of the broken symmetry<sup>2</sup>.

Our goals are similar to these. We hope to identify relevant coordinates and a corresponding effective theory. Experience has shown that an analytic approach is very difficult. The Villain form of the U(1) action yields some analytic results<sup>3</sup>, but the Wilson form for U(1) and SU(N) has not. Lattice simulations are capable of building evidence for or against this picture and perhaps even be a guide for analytic efforts.

The dual London relation found in pure gauge  $U(1)^4$  and  $SU(N)^{5,6}$  simulations gives evidence that an effective lattice dual Higgs theory is a credible candidate mechanism for confinement.

Fields and currents exist only near the boundaries of dual superconductors over a distance scale set by the London penetration depth  $\lambda_d$ . It is these spatially transient effects that provide spatial structures where the local properties of dual superconductivity can be studied and that is the focus of this work. A dual Abrikosov vortex is an example of such a structure. The core is ‘normal material’ and the flux tube connecting quark and antiquark is a spacially transient boundary effect.

## 2. Abrikosov vortices in the lattice Higgs effective theory

I would like to review briefly the salient features of the lattice Higgs theory in the tree approximation. It is relevant to note that in this model, the London relation is a direct consequence of the spontaneous breaking of the  $U(1)$  gauge theory. We compare the simulations of pure gauge theories with the dual of this model.

Consider the lattice action in a standard notation:

$$S = \beta \sum_{x, \mu > \nu} (1 - \cos \theta_{\mu\nu}(x)) - \kappa \sum_{x, \mu} (\phi^*(x) e^{i\theta_\mu(x)} \phi(x + \epsilon^{(\mu)}) + H.c.) + \sum_x V_{Higgs}(|\phi(x)|^2). \quad (1)$$

We are interested how the fields and currents respond to a magnetic monopole anti-monopole pair. We obtain a classical solution by minimizing the action. Our initial configuration contains a single closed magnetic monopole loop in the  $x_3, x_4$  plane analogous to the Wilson loop projector in the pure gauge simulations. Our algorithm then rejects all updated links that change the initial monopole configurations. We use the method of simulated annealing, slowly increasing  $\beta$ , holding  $\lambda^2/a^2 = \beta/\kappa = 1/e^2\kappa$  constant, where  $\lambda/a$  is the London penetration depth in lattice units and  $a$  is the lattice spacing.

The electric current is given by

$$\frac{a^3}{e\kappa} J_\mu^e(x) = \text{Im}(\phi^*(x) e^{i\theta_\mu(x)} \phi(x + \epsilon^{(\mu)})). \quad (2)$$

Writing the Higgs field  $\phi(x) = \rho(x) e^{i\omega(x)}$ , the curl of the current is hence given by

$$\begin{aligned} \frac{a^4}{e\kappa} (\Delta_\mu J_\nu^e(x) - \Delta_\nu J_\mu^e(x)) = & \\ & \rho(x) \rho(x + \epsilon^{(\mu)}) \sin[-\omega(x) + \theta_\mu(x) + \omega(x + \epsilon^{(\mu)})] + \\ & \rho(x + \epsilon^{(\mu)}) \rho(x + \epsilon^{(\mu)} + \epsilon^{(\nu)}) \sin[-\omega(x + \epsilon^{(\mu)}) + \theta_\nu(x + \epsilon^{(\mu)}) + \omega(x + \epsilon^{(\mu)} + \epsilon^{(\nu)})] - \\ & \rho(x + \epsilon^{(\nu)}) \rho(x + \epsilon^{(\nu)} + \epsilon^{(\mu)}) \sin[-\omega(x + \epsilon^{(\nu)}) + \theta_\mu(x + \epsilon^{(\nu)}) + \omega(x + \epsilon^{(\mu)} + \epsilon^{(\nu)})] - \\ & \rho(x) \rho(x + \epsilon^{(\nu)}) \sin[-\omega(x) + \theta_\nu(x) + \omega(x + \epsilon^{(\nu)})], \end{aligned} \quad (3)$$

where  $\Delta_\mu$  is the lattice derivative. Compare this with the electromagnetic field tensor

$$ea^2 F_{\mu\nu} = \sin[\theta_\mu(x) + \theta_\nu(x + \epsilon^{(\nu)}) - \theta_\mu(x + \epsilon^{(\nu)}) - \theta_\nu(x)]. \quad (4)$$

If the U(1) gauge symmetry is spontaneously broken, these two quantities are equal which is the London relation. To be more precise: if (i)  $\rho$  is nonvanishing and independent of position (absorb the normalization into  $\kappa$ ) and (ii)

$$\sin[\theta + 2n\pi] \approx \theta, \quad (5)$$

then

$$\mathcal{F}_{\mu\nu} \equiv F_{\mu\nu} - \frac{a^2}{e^2\kappa}(\Delta_\mu J_\nu^e(x) - \Delta_\nu J_\mu^e(x)) = \frac{2\pi n}{e} \frac{1}{a^2} = ne_m \frac{1}{a^2}, \quad (6)$$

where  $\mathcal{F}_{\mu\nu}a^2$  is called the fluxoid and  $e_m$  is the Dirac monopole charge. Condition (i) is satisfied by the SSB potential

$$V_{Higgs}(|\phi(x)|^2) \Rightarrow |\phi(x)|^2 = 1, \quad (7)$$

and (ii) is satisfied if the lattice is a good approximation, yet still allowing singular configurations when  $n \neq 0$  giving the quantized fluxoid. (A Dirac string would act differently, adding  $2\pi n$  to both quantities.) A ‘mexican hat potential’ can also give the London relation but it would be violated if the plaquette is within the coherence length of a superconducting-normal boundary where the Higgs field has a non-vanishing gradient.

Eqn.6, together with Maxwell’s equations, gives the Meissner effect  $\vec{B} - \lambda^2 \nabla^2 \vec{B} = 0$ , where  $\lambda^2 = m_\gamma^{-2}$ ; infinite conductivity  $\vec{E} = \lambda^2 \Delta_4 \vec{J}$  (assuming  $\rho = 0$ ); and an Abrikosov vortex

$$B_z - \lambda^2 (\vec{\Delta} \times \vec{J})_z = n \frac{e_m}{a^2} \delta_{x_\perp, 0}^2. \quad (8)$$

Fig.1 shows the profile of the R.H.S. of eqn.(3) and eqn.(4) in the directions perpendicular to the  $5 \times 5$  magnetic monopole loop on a  $12^4$  lattice, with  $\beta/\kappa = 1$ . We used the constrained form of the Higgs potential, eqn.(7), which corresponds to an extreme type II superconductor. The graphs show the expected behavior: i.e. the equality of the two quantities everywhere except at  $r = 0$  where they should differ by  $2\pi$ . There are significant violations only at  $r = 0$  and 1 due to the breakdown of Eqn. (5).

Lattice artifacts can violate the London and fluxoid quantization relations. But ignoring these controllable effects, the interior surface spanned by the monopole loop is in the normal phase since the London relation is violated there. All other regions are superconducting. This translates in the following sections in which the Wilson loop projects out the normal phase in the plane spanned by the loop and the remaining regions are a dual superconductor.

### 3. Dual superconductivity in pure U(1) gauge theory

We now turn to the dynamical simulations in pure U(1) gauge theory given by the

Fig. 1. Profile of  $ea^2F_{12}(x)$ , eqn.(4), and  $-(a^4/e\kappa)(\Delta_1J_2^e(x) - \Delta_2J_1^e(x))$ , eqn.(3), as a function of distance perpendicular to the plane of the monopole current loop in lattice units.

first term in the action, eqn.(1). We have given evidence in ref.<sup>4</sup> that a dual London relation is satisfied:

$$\mathcal{G}_{\mu\nu} \equiv \frac{1}{2}\epsilon_{\mu\nu\sigma\tau}F_{\sigma\tau} - \lambda_d^2(\Delta_\mu J_\nu^m(x) - \Delta_\nu J_\mu^m(x)) = \frac{ne}{a^2}\delta_{x_\mu,0}\delta_{x_\nu,0}. \quad (9)$$

Magnetic monopoles are the current-carriers responsible for the dual superconductivity. These monopoles are defined in a 3-volume by the DeGrand-Toussaint<sup>7</sup> construction, separating multiples of  $2\pi$  from the plaquette angle,  $(-\pi < \bar{\theta}_{\mu\nu}(x) \leq \pi)$ :

$$\theta_{\mu\nu}(x) = \bar{\theta}_{\mu\nu}(x) + 2\pi n_{\mu\nu}(x); \quad J_\mu^m(x) = \epsilon_{\mu\nu\sigma\tau}(\bar{\theta}_{\sigma\tau}(x + \epsilon^{(\nu)}) - \bar{\theta}_{\sigma\tau}(x)) \quad (10)$$

We associate  $J_\mu^m(x)$  with a link on the dual lattice, making world lines which define a conserved current density. The key idea is to measure the line integral of  $J_\mu^m$  around a dual plaquette, giving  $a^2(curl J^m)_{\mu\nu}$ . The correlation of this with a Wilson loop, gives a signal for the solenoidal behavior of the currents surrounding the electric flux between oppositely charged particles.

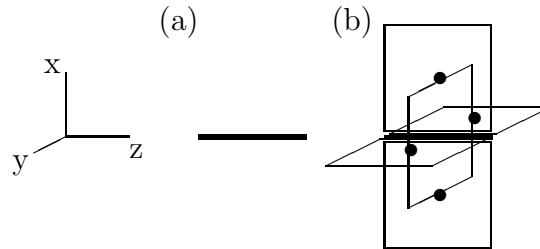


Fig. 2. Operators for (a)  $ea^2F_{34}(x)$ , and (b)  $(a^4/e_m)(\Delta_1J_2^m(x) - \Delta_2J_1^m(x))$ .

Fig. 2 shows the lattice operators for the electric field and the curl of the magnetic monopole current. The longitudinal electric field, (a), is given by a  $z, t$  plaquette which is depicted by a bold line for fixed time. The curl of the magnetic monopole

Fig. 3. Profile of  $ea^2F_{34}(x)$  and  $-(a^4/e_m)(\Delta_1 J_2^m(x) - \Delta_2 J_1^m(x))$  as a function of distance perpendicular to the plane of the Wilson loop in lattice units.

current, (b), is built from four 3-volumes which appear as squares since the time dimension is not shown. Passing through the center of each square is the link dual to the 3-volume. One takes the monopole number  $n$  in each 3-volume and associates the value  $ne_m$  with the corresponding dual link. The ‘line integral’ around the dual plaquette completes the picture. Notice from this construction that  $\vec{E}$  and  $\vec{\Delta} \times \vec{J}^m$  take values at the same location within the unit cell of the lattice, both are indicated by the bold face line in the  $z$  direction. Both operators are in defined on the same  $z, t$  plaquette.

Fig.3 shows the profile for the quantities making up the London relation on the same plot as for the effective lattice Higgs case, Fig.1. We did 800 measurements on a  $12^4$  lattice,  $\beta = 0.95$ , and a  $3 \times 3$  Wilson loop was used to project onto the  $q, \bar{q}$  sector using methods described in Ref.(4). We did a  $\chi^2$  fit of the London relation, eqn.(9), using the  $r \neq 0$  points and determined  $\lambda_d = 0.49(3)$ . that determined the coefficient of the delta function in eqn.(9),  $ne = 1.07(7)$ , compared to the expected value  $1/\sqrt{\beta} = 1.03$ . All these features correspond directly to the classical solution of the lattice Higgs model reinterpreted as a dual theory.

#### 4. Generalization to pure SU(2) and SU(3) gauge theories

In ref.(5) we applied these same techniques and showed that dual Abrikosov vortices also occur in SU(2) pure gauge theory in the maximal Abelian gauge. Matsubara et.al.<sup>6</sup> confirmed these results with better statistics and generalized them to SU(3). The SU(2) link matrices are  $U_\mu(x)$  and the action is

$$S = \beta \sum_{x, \mu > \nu} (1 - \frac{1}{2} \text{Tr} U_{\mu\nu}(x)). \quad (11)$$

The maximal Abelian gauge is defined by maximizing the quantity

$$R = \sum_{x, \mu} \text{Tr} [\sigma_3 U_\mu(x) \sigma_3 U_\mu^\dagger(x)]. \quad (12)$$

Fig. 4. Same plot as in fig.3 but for SU(2), in the confined phase

Fig. 5. Same plot as in fig.3,4 but for SU(2), in the deconfined phase.

The Abelian link angle is then taken as the phase of  $[U_\mu(x)]_{11}$  and the calculation can proceed with little change<sup>8</sup>.

Recently we have done the calculation at finite temperature in order to check this picture on each side of the deconfining phase transition<sup>9</sup> which we report here. The results are shown in the confining phase, fig.4,  $\beta = 2.28$  and the deconfining phase, fig.5,  $\beta = 2.40$  on a lattice  $4 \times 17^2 \times 19$ , with 800 measurements for each case. Gauge fixing required about 600 sweeps for each configuration. Fig.4 shows an important difference from the U(1) case. Whereas in the U(1) case a linear combination of  $E$  and  $curl J^m$  for  $r \neq 0$  can vanish giving the London relation, it is clearly not possible here. The behavior of  $-curl J^m$  does not match that of  $E$ . We interpret this discrepancy as a signal of a non-zero Ginzburg-Landau coherence length,  $\xi_d$ . Whereas all evidence in the U(1) case points to the extreme type II limit, i.e. the superconducting order parameter turning on at the surface, the evidence here is that the order parameter turns on with a behavior  $\tanh(x_\perp/\xi_d)$ . The value of the coherence length is approximately the radius where the London relation is restored.

The simulation shown in fig.5 was identical to fig.4 except that  $\beta$  was increased to 2.40 putting us in the deconfining phase. The dramatic decrease of  $curl J^m$  results in the failure of the dual superconductor interpretation as expected for the deconfining phase. Also  $E$  falls more slowly with radius.

The behavior of all the SU(2) and SU(3) examples is similar to that shown in fig.4.

The interesting conclusion is that  $\kappa_d \equiv \lambda_d/\xi_d \approx 1$  (no relation to Higgs  $\kappa$ ) For a type II dual superconductor  $\kappa_d > 1/\sqrt{2}$  and a type I otherwise. These simulations indicate that the non-Abelian dual superconductors lie at the borderline between type I and type II. However a more systematic study is needed to pin this down.

## 5. External Electric Field

Many interesting superconducting properties can be elucidated by studying the properties of the material in the presence of a magnetic field. We report a preliminary look at the corresponding problem of dual superconductivity in the presence of an external electric field. The Wilson loop provides such a field by projecting a  $q\bar{q}$  out of vacuum configurations. But it may be interesting to see the spontaneous breaking of translation invariance as the electric flux forms a vortex rather than impose the vortex position at a given location and with quantized flux. Type I and type II dual superconductors respond very differently to background uniform external fields.

For a periodic U(1) lattice the sum of the plaquette angles over any plane is identically zero. A classical uniform electric field for U(1) on a particular time slice can still be obtained by constraining one plaquette angle in each  $z, t$  plane to the value  $(1/(N_z N_t) - 1)\theta_c$ . Then the remaining  $(N_z N_t - 1)$  plaquette angles will take the common value  $\theta_c/(N_z N_t) = ea^2 F_{34}$  giving a uniform electric field on all but one time slice. (N labels the lattice dimensions.) Choosing  $\theta_c = \pi$  gives the largest field. For an  $8^4$  lattice and  $\beta = 1$  for example, there would be enough electric flux to form about 3 vortices in the  $x, y$  plane in the dual superconducting phase. This field configuration can also be obtained by multiplying the plaquette that was singled out in the action by a minus sign and such configurations have been studied in non-Abelian theories<sup>10</sup>. We avoided an alternative method of imposing an external field by introducing a non-zero equilibrium value locally for each plaquette angle since we eventually want to see the field break translation invariance. Turning on interactions for  $\beta < 1$  brings up other interesting features<sup>11</sup>.

Our goal here is to try to see a signal showing that  $curl J^m$  responds to the external field. The immediate problem is that the sum of  $(curl J^m)_{xy}$  over the any  $x, y$  plane is identically zero, and the sum of  $E_z$  is not. Yet we expect the London relation to be satisfied. The only possibility is that translation invariance is broken which is expected since vortices segregate the superconducting and normal phases.

We make the following rough ansatz that the local London relation is due to a the alignment of local current loops in the external field. This suggests that we truncate  $curl J^m$  to include only values  $\pm 2, \pm 3, \pm 4$  representing the winding of the current around the dual plaquette. We denote this  $J_\mu^m(2 + 3 + 4)$ .

Now we get a large signal for  $curl J_\mu^m(2 + 3 + 4)$  as shown in fig.6 with a sign that agrees with the sign in fig.3 for the superconducting region,  $r \neq 0$ . Further if we recalculate fig.3 with the truncated current, we find a large suppression at  $r = 0$

Fig. 6. Average of  $ea^2F_{34}$  and  $-(a^4/e_m)(\Delta_1 J_2^m(2+3+4) - \Delta_2 J_1^m(2+3+4))$  on each time slice for an external field  $= \pi/64$  (the horizontal line). The constrained plaquette is at  $t = 1$ , the field is classical at  $t = 2, 8$  and  $\beta = .99$  for  $t = 3 - 7$ .

and a moderate enhancement at the other points. In other words this choice biases in favor of the dual superconducting phase.

## 6. Acknowledgements

I wish to thank D. Browne, L.-H. Chan, A. Di Giacomo, Y. Peng, M. Polikarpov, H. Rothe, G. Schierholz, V. Singh, J. Wosiek, and K. Yee for many discussions. We are supported in part by the US Department of Energy grant DE-FG05-91ER40617.

## 7. References

1. H.B. Nielsen and P. Olesen, Nucl. Phys. **B61** (1973) 45; S. Mandelstam, Phys. Rep. **23** (1976) 245; G. 'tHooft in High energy physics, ed. A. Zichichi (Editrice Compositori, Bologna, 1976).
2. M. Tinkham, Introduction to superconductivity, (McGraw-Hill, New York, 1975).
3. T. Banks, R. Myerson, and J. Kogut, Nucl. Phys. **B129**, (1977) 493.
4. V. Singh, R.W. Haymaker, and D.A. Browne, Phys. Rev. **D47**, (1993) 1715.
5. V. Singh, D.A. Browne, and R.W. Haymaker, Phys. Lett. **B306** (1993) 115.
6. Y. Matsubara, S. Ejiri, and T. Suzuki, Nucl. Phys. **B34** (Proc. Suppl.) (1994) 176.
7. T. A. DeGrand and D. Toussaint, Phys. Rev. **D22** (1980) 2478.
8. A.S. Kronfeld, G. Schierholz and U.-J. Wiese, Phys. Lett. **B198** (1987) 516; A.S. Kronfeld, M.L. Laursen, G. Schierholz and U.-J. Wiese, Nucl. Phys. **B293** (1987) 461; T. Suzuki and I. Yotsuyanagi, Phys. Rev. **D42** (1990) 4257; J. Smit and A. J. van der Sijs, Nucl. Phys. **B355** (1991) 603; T.L. Ivanenko, A.V. Pochinsky and M.I. Polikarpov, Phys. Rev. Lett. **B252** (1990) 631.
9. Y. Peng and R.W. Haymaker, LSU preprint LSUHE No. 183-1994.



10. A. Gonzalez-Arroyo and M. Okawa, Phys. Lett. **120B**, (1983) 174.
11. P.H. Damgaard and U.M. Heller, Phys. Rev. Lett. **60** (1988) 1246.